JOURNAL OF MATERIALS SCIENCE 26 (1991) 5979–5984

Structure and thermal evolution of mullite aerogels

F. CLUZEL, G. LARNAC, J. PHALIPPOU
Laboratoire de Science des Matériaux Vitreux (U.A. 1119), Université de Montpellier II, 34095 Montpellier Cedex, France

Gels with mullite composition have been prepared from pseudo-boehmite sol and tetramethoxysilane. They are then converted to aerogels using methanol or CO_2 supercritical drying. The structure of the aerogels depends on the nature of the solvent used to perform the hypercritical solvent evacuation. Infrared spectroscopy shows that an esterification reaction occurs during the methanol supercritical drying. The samples prepared by CO_2 supercritical drying retain some isoamylacetate, which is used to exchange solvent. Small angle neutron scattering experiments lead to the conclusion that aerogels prepared with either supercritical drying technique are constituted by primary particles of equal size, and are characterized by the same volume fractal dimension. The thermal evolution of a monolithic methanol evacuated sample leads to cracks free ceramic having an apparent density of 1.1 and which does not evolve when heat treated below 1200 °C.

1. Introduction

Mullite ($3Al_2O_3$–$2SiO_2$) is a high temperature binary oxide. For many applications mullite is often preferred to alumina because of its lower thermal expansion coefficient and density [1, 2].

This type of material is used as a thermal insulator because of its refractoriness. In that case, thermal insulation properties can be enhanced by porosity [3]. Apart from the usual foam ceramics a new class of insulator materials is now being studied. These materials are prepared from gels and called aerogels in respect to the manner to dry them.

Aerogels are mostly amorphous and crystallization occurs in competition with sintering. If crystallization happens before the aerogel has been densified, the stresses induced by the dimensional changes due to crystallization may cause cracks. In this respect it may be useful to partially densify the aerogel at low temperature in order to reinforce its backbone.

It was previously demonstrated that densification of mullite gel occurs at lower temperature when the starting gel is not homogeneous but consists of small heterogeneous particles of 10 nm size [4–9].

In that case, however, the starting microstructure should be carefully controlled in such a way to avoid a final heterogeneous microstructure consisting of mullite, silica (amorphous or cristobalite) and alumina.

Pure mullite compound seems to be obtained from a mixture of pseudo-boehmite sol and an organosilicon compound.

We report here the study of the structure of two different kinds of mullite aerogels obtained from CO_2 or methanol evacuation. Their morphology is analysed in terms of fractal concepts. The thermal evolution of these aerogels is followed using dilatometric measurements.

2. Experimental procedure

Mullite gels were prepared from a pseudo-boehmite sol [10] and from tetramethoxysilane (TMOS) diluted in methanol. The alumina sol is aged for ten days to allow the setting of the largest aggregates. The upper solution is then removed and can be concentrated by a gentle solvent evaporation. The maximum alumina content of the solution corresponds to 1 Al_2O_3 mol l^{-1}. TMOS was used because of its higher solubility in water as compared to tetramethoxysilane.

The starting solution is poured into a container which is then hermetically closed and heat-treated at 40 °C. In such conditions gelation occurs in a few hours. Ageing of the gel is carried out at the same temperature for one week. A crack-free gel is obtained. The liquid part of the gel is mainly constituted by water, thus a washing of the gel is necessary to remove this solvent. Obviously, when the gel is submitted to high temperature and high pressure treatments, water acts as a mineralizer and leads to crystallization of silica. The gel is washed with methanol. During the ageing treatment no shrinkage occurs and the gel is difficult to remove from its container. Washing is carried out continuously after removing the bottom part of the glass container (Fig. 1).

Due to the low permeability of gels [11] the solvent exchange takes two days. Such gels are supercritically dried using methanol as a solvent [12]. Another series of samples was submitted to a solvent exchange by amylacetate for one week by changing the bath every day. The last step of this solvent exchange was

0022–2461/91 $03.00 + .12

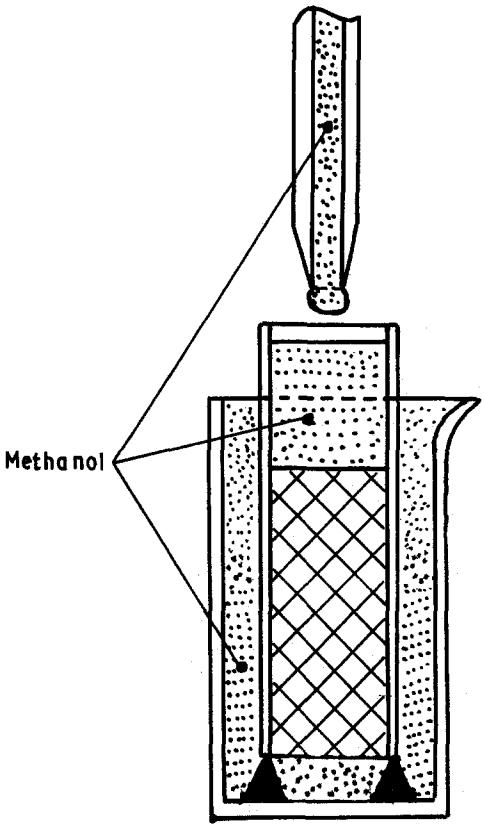

Figure 1 Washing mode of gel.

performed in the autoclave and consists of exchanging amylacetate with liquid CO_2. The exchange is performed for two days before the onset of the CO_2 supercritical drying.

Gels that are subjected to a lot of solvent exchanges are chemically analysed in respect to their expected chemical composition. On the other hand the silica content (compared to that of mullite) can have a significant influence on sintering temperature if it exceeds that of stoichiometric mullite.

Chemical analysis of mullite aerogel is performed using flame spectroscopy. Standard curves were established from solutions of given amounts of silica dissolved in a $HF–HNO_3$ mixture and from $AlNO_3$ solutions. The measurement is carried out as previously reported [13].

The apparent density of aerogels is measured by weighting monolithic samples having a perfectly defined geometry.

The structural analysis of aerogels is realized by IR spectroscopy on thin slice of monolithic aerogels. Textural properties of aerogels are measured using nitrogen adsorption–desorption isotherm curves. The specific surface area is measured by BET [14] and the pore size distribution by BJH [15].

Small angle neutron scattering (SANS) experiments were performed on the spectrometer PACE at the 'Laboratoire Leon Brillouin' in Saclay. Scattering vectors Q ranging from 0.018 to 3 nm^{-1} were covered ($Q = 4\pi \sin\theta/\lambda$; 2θ is the scattering angle). A standard analysis of data including detector efficiency correction, background substraction and relative amplitude calibration allows a determination of the density–density correlation function in the range 0.3 to 50 nm.

X-ray diffraction allows the structural evolution to be followed. The linear change of samples as a function of temperature is recorded with a dilatometer. This technique only applies, however, to samples strong enough to withstand the stress induced by the push-rod.

3. Results and discussion

3.1. Structural properties

Fig. 2 shows the aspect of a monolithic mullite aerogel. The main macroscopic characteristics do not depend on the solvent used to carry out the supercritical drying. In both cases the linear shrinkage experienced by gels during the supercritical drying is very low (1%). A syneresis phenomenon is never observed. In this respect we expect that a further polycondensation reaction after the gelation point does not occur.

Such a behaviour was previously observed on base catalysed silica aerogels having a low solid content [16]. The low shrinkage was attributed to the morphology of the solid part of the material which was constituted by an assembly of large size primary units strongly linked together.

The aerogel density is very low and mainly depends on the alumina sol concentration (Table I). Lighter monolithic aerogels can be obtained. They do not, however, withstand their own weight due to their low strength.

Chemical analyses of aerogels M (methanol evacuated) and aerogels C (CO_2 evacuated) have been performed on 1300 °C treated samples. The deduced chemical composition approximately corresponds to stoichiometric mullite (Table II). Consequently the different solvent exchanges do not induce any dissolution of the chemical elements constituting the solid part of the gel.

X-ray diffraction patterns demonstrate that the structure of aerogels M and C is identical. Aerogels consist of pseudo-boehmite [17] and amorphous silica. Some difference in the structure can, however, be seen from IR spectroscopy (Fig. 3).

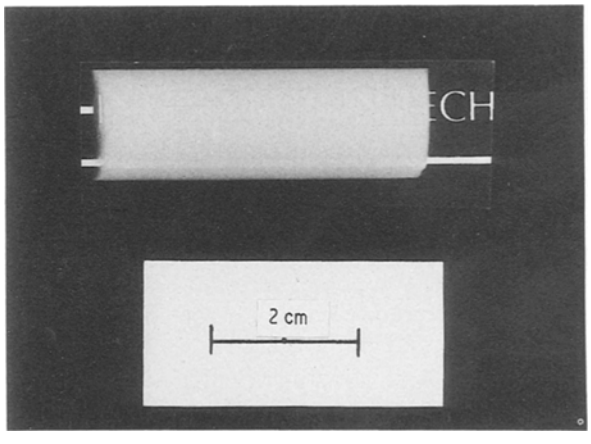

Figure 2 Methanol evacuated mullite aerogel.

TABLE I Density of methanol (M) evacuated and CO_2 (C) evacuated mullite aerogels

Code	Boehmite sol (cm^3) (mole Al_2O_3 l)	Apparent density ($g\,cm^{-2}$)
M_1	0.61	0.07
M_2	0.78	0.086
M_3	0.83	0.097
C	0.83	0.089

TABLE II Chemical analysis of mullite aerogels

	Silica (wt %)	Alumina (wt %)
Mullite crystal	28.17	71.83
Aerogel M_1	29.19	70.81
Aerogel M_2	29.2	70.8
Aerogel C	29.8	70.2

The two sharp bands located at 3295 and 3090 cm^{-1} (Fig. 3a) are assigned to OH vibrations of boehmite [18]. They emerge from a broad band which is attributed to the different hydroxyl groups usually found in silica gels. The bending vibration associated with stretching OH of boehmite can not be observed (1060 cm^{-1}) because it appears in a spectral range corresponding to the Si–O–Si stretching vibration. The IR bands located around 775, 610 cm^{-1} are due to stretching vibrations of (AlO_6) units. The 482 cm^{-1} band is assigned to Si–O–Si bending vibration [19]. The bending vibration of (AlO_6) units is located at 360 cm^{-1}.

The IR spectrum of the mullite aerogel M is similar to that of a pseudo-boehmite xerogel [20]. The appearance of a well defined band located around 2850 cm^{-1} indicates, however, the presence of OCH_3 group linked to silicon atom. In respect to this absorption band two main hypotheses can be proposed: the hydrolysis of TMOS is not fully achieved or an esterification reaction takes place during the hypercritical drying process.

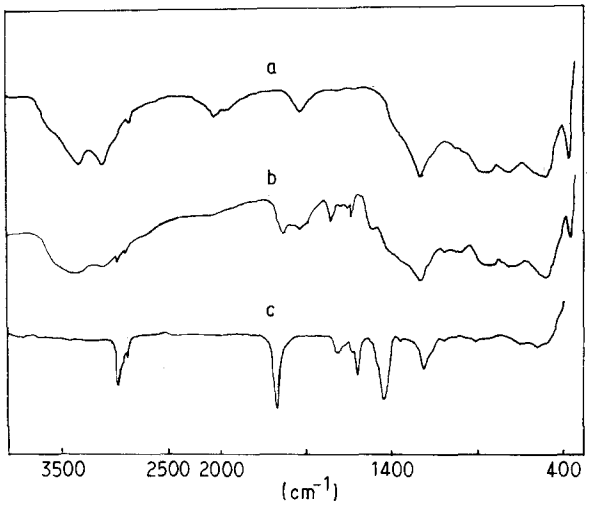

Figure 3 IR spectra of (a) aerogel M, (b) C and (c) isoamylacetate compound.

Due to the large amount of water contained in the alumina sol, the hydrolysis of TMOS is likely to be complete. On the other hand, it was previously demonstrated that hydroxyl groups linked to aluminium atoms do not undergo an esterification reaction when reacted with an alcohol [21]. Consequently the expected esterification reaction only takes place on surface silanols. The respective IR bands of these species are located at 2940, 2840 and 1455 cm^{-1}. In our samples only the 2840 cm^{-1} band is observed, thus the extent of the esterification reaction of the aerogel surface is very low and does not induce an hydrophobicity of the material. This is confirmed by the presence of the 1620 cm^{-1} assigned to bending vibration of water molecules.

The IR spectrum of the aerogel C (Fig. 3b) does not show the previous band located at 2840 cm^{-1}. As expected, this other way of performing supercritical drying does not induce a chemical reaction of surface esterification. This kind of aerogel is thus particularly hydrophilic as demonstrated by IR bands located around 3500 and 1620 cm^{-1}. Moreover new absorption bands, which are most intense at 2940, 2880, 1710, 1470, 1375 and 1290 cm^{-1} are observed. The location of these bands approximately corresponds to an amylacetate compound (Fig. 3c). Nevertheless the absorption bands located at 1740 and 1240 cm^{-1} are shifted comparatively to pure amylacetate. This feature confirms that an association occurs between the solvent and the aerogel backbone.

The exchange of amylacetate by liquid CO_2 can not be totally achieved. Even if the exchange takes longer than two days the IR spectrum of the aerogel reveals the presence of isoamylacetate. This phenomenon is probably linked to a strong tendency of isoamylacetate to adsorb on mullite aerogels. It is noteworthy that this phenomenon was not observed on previously prepared pure silica CO_2 evacuated aerogels [22, 23].

The adsorption–desorption curves (Fig. 4a and b) allow the specific surface area to be evaluated. The obtained values are close to those of pure boehmite aerogels [24]. The type of curve where the isotherm does not reach a well defined limit when P/P_s approaches 1, is usually observed for materials showing a simple surface adsorption; the total filling of the pores never occurs. The desorption curve exhibits a very low hysteresis effect (type 2 according to the BET nomenclature).

The analysis of these curves brings information on the cumulated porous volume in the pore radius range between 2 and 13 nm. The cumulated porous volume of aerogels is a lot smaller than the total porous volume evaluated from the apparent density. Consequently the macroporous volume of the aerogel is rather large.

The comparison between the cumulated porous volume of C (Fig. 5a) and M (Fig. 5b) aerogels shows a few differences. The cumulated porous volume reaches 40% for aerogel C while it is about 80% for aerogel M. This feature is probably linked to the initial presence of isoamylacetate in the pores of the aerogel which develops stresses high enough to induce cracks of mesopores. The adsorption desorption isotherms

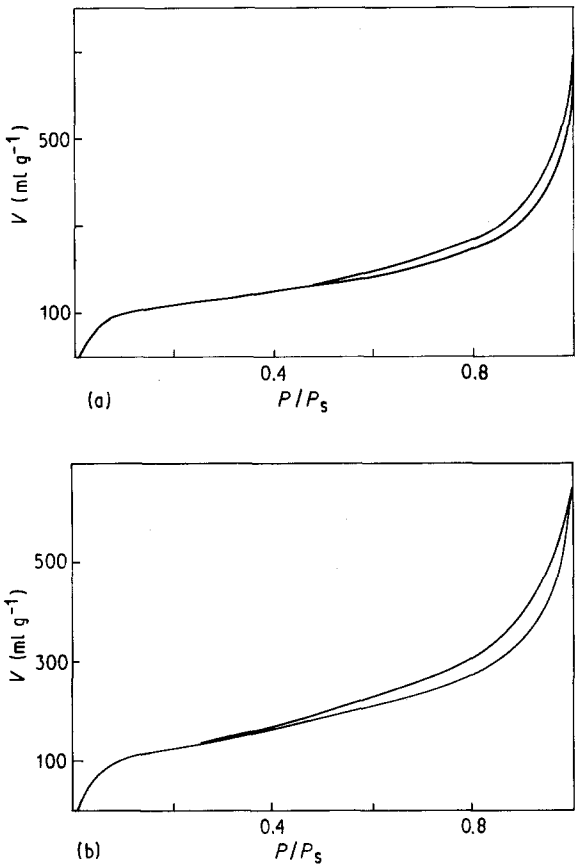

Figure 4 Nitrogen adsorption–desorption isotherms. (a) aerogel C; (b) aerogel M.

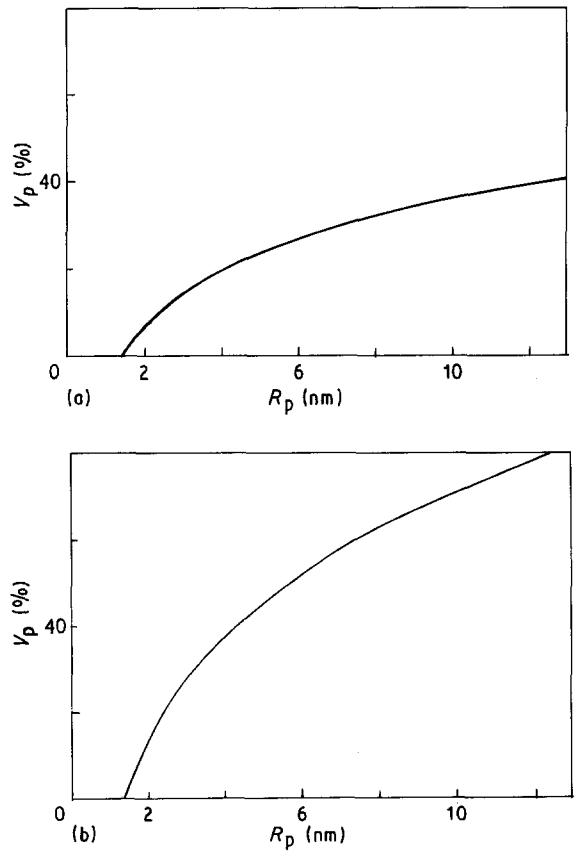

Figure 5 Cumulated pore volume as a function of pore radius. (a) aerogel C; (b) aerogel M.

are, however, performed on outgassed materials, thus isoamylacetate does play a direct role on textural properties.

Small angle neutron scattering curves have been studied in terms of fractal analysis. The aerogel is considered to be made up of dense small particles spatially distributed in a fractal manner. Small angle neutron scattering experiments were carried out on samples maintained at a temperature of 90 °C to avoid water and to remove most adsorbed species.

The pair correlation function and the probability of finding a particle at a distance R from a reference particle have previously been reported [25]. The authors introduced a cut-off to take into account the limited fractal range of a real material. The material is no more fractal for a scale length higher than the correlation length ξ. The Fourier transform of the pair correlation permits the variation of the scattered intensity $I(Q)$ as a function of the vector wave Q to be calculated.

For a fractal object $I(Q) \alpha Q^{-D}$ when $1/\xi < Q < 1/r_0$ where D is the volume fractal dimension and r_0 the size of the primary particle. On the other hand for $Q \ll 1/\xi$ the scattered intensity obeys the classical Guinier's equation [26].

On the high Q side the log–log plot of intensity as a function of vector wave shows a slope equal to -4 for aerogel C (Fig. 6a). In this Q domain the slope is related to a hypothetical fractal surface dimension D_s by the relation

$$\text{slope} = D_s - 6$$

For a non-surface fractal material D_s is equal to 2 and the Porod's law is relevant. Consequently the particles constituting the aerogel C are not rough and the interface between particles and air is smooth.

Conversely the aerogel M (Fig. 6b) shows a fractal surface ($D_s \simeq 3$) coming from the esterification

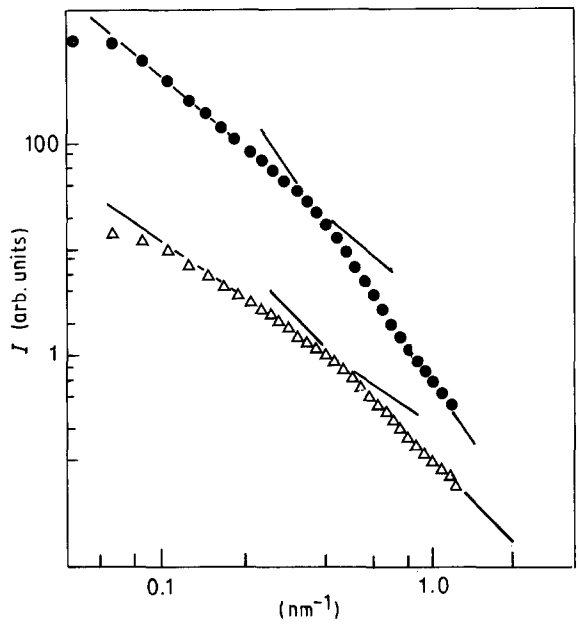

Figure 6 Small angle neutron scattering curves for aerogels C (●) and M (△) (curves are shifted for clarity).

reaction induced by the autoclave treatment. An analogous behaviour has been found on pure silica aerogels [27].

Using fractal analysis an assumption is often made to evaluate the gyration radius, a, of particles. It is expected to correspond to the cross-over between the regimes: volume fractality–surface fractality or Porod's behaviour. With this assumption the gyration radius is identical for the two sorts of aerogels and evaluated to 2.5 nm.

As indicated above, the slope of the curves, in the domain $Q < 1/a$, gives the volume fractal dimension. For both materials the fractal dimension is 2.3. A correlation of the obtained fractal dimension with that evaluated using fractal models of aggregation is not straightforward because of the structural evolution from the gel to the aerogel. The observed fractal dimension is, however, in good agreement with the reaction limited cluster aggregation model [28].

Results of SANS experiments lead to the conclusion that the volume fractal dimension which is related to the volume occupied by the solid part is not dependent on the way the aerogels are obtained.

3.2. Thermal evolution of aerogels

X-ray diffraction experiments have been carried out to follow the structural evolution of aerogels as a function of temperature. To perform this study the samples were heat treated for 1 h at a given temperature. Because of their hydrophilic property they were maintained at 90 °C until their analysis.

Aerogel M is a diphasic material constituted by pseudo-boehmite and amorphous silica (Fig. 7). At 550 °C pseudo-boehmite transforms into γ-Al_2O_3. Cristobalite appears at a temperature of about 1000 °C. Between 1175 and 1225 °C the XR pattern corresponds to δ-Al_2O_3, cristobalite and a residual amorphous silica compound which causes a diffuse halo. Mullite appears at 1250 °C while cristobalite is still present. The crystallization sequency of aerogel M is in good agreement with other reported studies [29, 30]. α-Al_2O_3 is never formed because γ-alumina reacts with silica to make mullite. For temperatures higher than 1300 °C the X-ray diffraction pattern indicates the presence of a small amount of cristobalite.

The thermal evolution of aerogel C is identical to that observed on aerogel M. When heat treated at 1300 °C the aerogel C is, however, fully transformed into pure mullite (Fig. 8). This difference is not presently well understood. Small deviations from the stoichiometric composition can not account for the observed effect. This difference would be linked to the drying mode experienced by the gels.

The most dense sample of aerogel M has been studied using dilatometric measurement. A shrinkage of a small extent first appears at about 400 °C (Fig. 9). It is located in a temperature range corresponding to the pseudo-boehmite–γ-alumina transformation. At higher temperature, the sintering is very fast and is

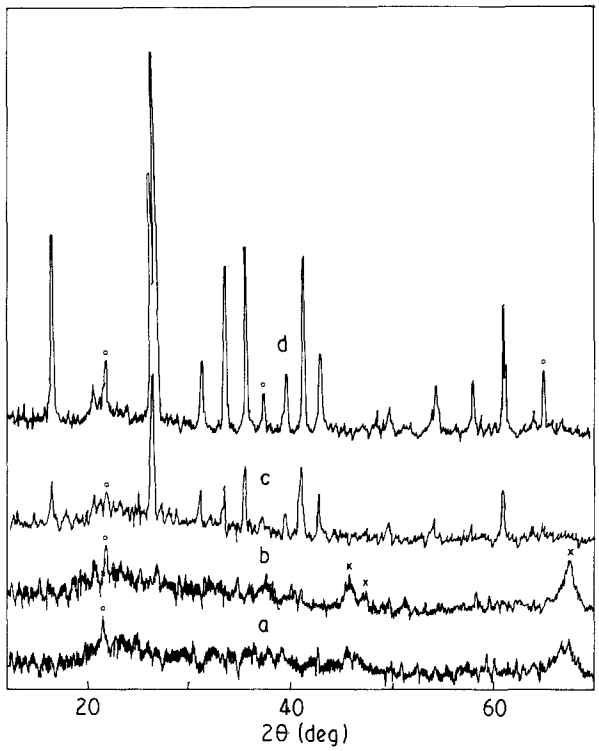

Figure 7 XR diffraction of aerogel M as a function of temperature. The duration of heat-treatment is 1 h. (a 1000 °C, b 1225 °C, c 1250 °C, d 1275 °C. ○ refers to cristobalite; × to δ Al_2O_3.)

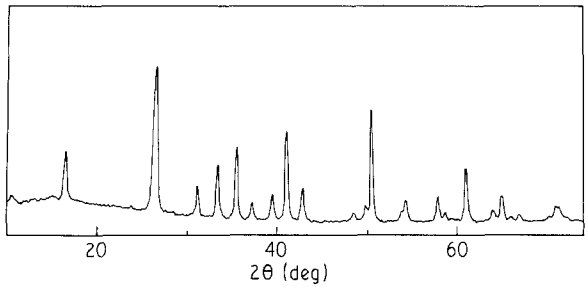

Figure 8 XR diffraction pattern of fully crystallized aerogel C.

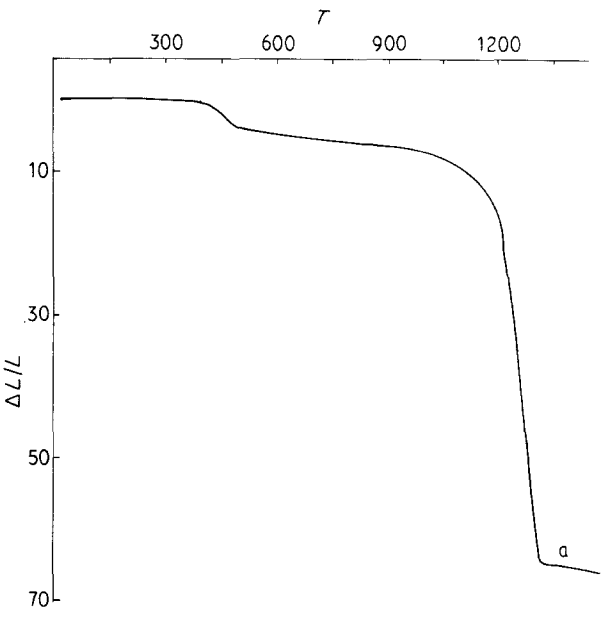

Figure 9 Linear shrinkage of monolithic aerogel M.

probably due to a viscous flow phenomenon provoked by amorphous silica.

Densification suddenly stops, however, as soon as mullite appears. The end of the rapid densification occurs at about 1300 °C. Above this temperature sintering slightly continues by a diffusion phenomenon whose rate is very low.

It is important to note that during the whole run (heating up and cooling down) the material retains its monolithic shape. The aerogel whose initial apparent density is 0.097 is converted to ceramic material having an apparent density of 1.2. The porosity is totally open. The mean pore size is probably lower than 1 μm as found in other usual aerogel.

4. Conclusions

Microheterogeneous aerogels with a composition close to mullite were prepared. The supercritical drying was carried out using two different liquids. The structure of aerogels as characterized by IR spectroscopy depends on the supercritical drying process. Methanol evacuated samples have undergone an esterification reaction. This reaction which only takes place on surface silanol groups does not, however, result in a hydrophobic material. CO_2 evacuated samples retain in their pores a small amount of isoamylacetate which is the liquid used to carry out the solvent exchange before CO_2 drying.

SANS experiments lead to the conclusion that both aerogels are constituted by identical elementary particles linked together in the same manner. The volume fractal dimension is identical. Nevertheless the esterification reaction occurring in aerogel M causes a surface roughness inducing a deviation from Porod law.

Both aerogels are very fragile and lightweight. The most dense are able to sustain their own weight without strain. They were heat treated and transformed into highly porous ceramic materials which can be used as monolithic insulator at temperature lower than 1300 °C.

Acknowledgements

The authors are grateful for the financial support of Delegation des Recherches Etudes et Techniques.

References

1. W. D. KINGERY, H. K. BOWEN and D. R. ULHMANN, "Introduction to ceramics", 2nd Edn (Wiley, New York 1976).
2. A. J. SKOOG and R. E. MOORE, *J. Amer. Ceram. Soc. Bull.* **67** (1988) 1180.
3. S. K. MAITI, L. J. GIBSON and M. F. ASHBY, *Acta Metall.* **32** (1984) 1963.
4. B. E. YOLDAS and D. P. PARTLOW, *J. Mater. Sci. Lett.* **23** (1988) 1895.
5. K. OKADA, Y. HOSHI and N. OTSUKA, *ibid.* **5** (1986) 1376.
6. D. W. HOFFMAN, R. ROY and S. KOMARNENI, *J. Amer. Ceram. Soc.* **67** (1984) 468.
7. S. KOMARNENI, Y. SUWA and R. ROY, *ibid.* **69** (1986) C155.
8. J. A. PASK, X. W. ZHANG, A. P. THOMSIA and B. E. YOLDAS, *ibid.* **70** (1987) 704.
9. M. G. M. U. ISMAIL, Z. NAKAI and S. SOMIYA, *ibid.* **70** (1987) C7.
10. B. E. YOLDAS, *Amer. Ceram. Soc. Bull.* **54** (1975) 289.
11. G. W. SCHERER, *J. Non-Cryst. Solids* **109** (1989) 183.
12. J. PHALIPPOU and T. WOIGNIER, M. PRASSAS, *J. Mater. Sci.* **25** (1990) 311.
13. W. P. KILBOY and C. T. MOYNIHAN, *Amer. Ceram. Soc. Bull.* **57** (1978) 1034.
14. S. BRUNAUER, P. H. EMMETT and E. TELLER, *J. Amer. Chem. Soc.* **60** (1938) 309.
15. E. P. BARRET, L. G. JOYNER and P. P. HALENDA, *ibid.* **73** (1951) 373.
16. T. WOIGNIER, J. PHALIPPOU, H. HDACH and G. W. SCHERER, "Better ceramic through chemistry IV", *Mat. Res. Soc. Symp. Proceedings*, Vol. 180, San Francisco, April 1990, edited by C. J. Brinker, D. E. Clark and D. R. Ulrich (Material Research Society, Pittsburgh, 1990) p. 1087.
17. D. PAPEE, R. TERTIAN and R. BIAIS, *Bull. Soc. Chim. Fr.* (1958) 1301.
18. T. SATO, *Z. Anorg. Chem.* **391** (1972) 167.
19. A. B. KISS, G. KERESZTURY and L. FARKAS, *Spectrochim. Acta* **36A** (1980) 653.
20. T. ASSIH, A. AYRAL, M. ABENOZA and J. PHALIPPOU, *J. Mater. Sci.* **23** (1988) 3326.
21. J. FRIPIAT, J. CHAUSSIDON and A. JELLI, "Chimie-physique des phénomènes de surface" (Masson, Paris, 1971) p. 305.
22. P. H. TEWARI, A. J. HUNT and K. D. LOFFTUS, *J. Mater. Sci. Lett.* **3** (1985) 363.
23. J. PHALIPPOU, T. WOIGNIER and M. PRASSAS, *Rev. Phys. Appl.* **C4** (1989) 47.
24. S. M. WOLFRUM, *J. Mater. Sci. Lett.* **6** (1987) 706.
25. S. K. SINHA, T. FRELOFT and J. KJEMS, "Kinetics of aggregation and gelation", edited by F. Family and D. P. Landau (Elsevier, Amsterdam, 1984) p. 87.
26. A. GUINIER and G. FOURNET, "Small angle scattering of X-rays" (John Wiley, New York, 1955).
27. R. VACHER, T. WOIGNIER, J. PELOUS and E. COURTENS, *Phys. Rev. B* **37** (1988) 6500.
28. M. KOLB, R. BOTET and R. JULLIEN, *J. Phys. Lett.* **45** (1984) 211.
29. W. C. WEI and J. W. HALLORAN, *J. Amer. Ceram. Soc.* **71** (1988) 166.
30. *Idem, ibid.* **71** (1988) 581.

Received 5 November 1990
and accepted 25 March 1991